JOC The Journal of Organic Chemistry

Article

Scorpionate Catalysts for Coupling CO2 and Epoxides to Cyclic Carbonates: A Rational Design Approach for Organocatalysts

Mannkyu Hong, Yoseph Kim, Hyejin Kim, Hee Jin Cho, Mu-Hyun Baik, and Youngjo Kim

J. Org. Chem., **Just Accepted Manuscript** • DOI: 10.1021/acs.joc.8b00722 • Publication Date (Web): 20 Jun 2018

ACS Publications

is published by the American Chemical Society. 1155 Sixteenth Street N.W., Washington, DC 20036

Scorpionate Catalysts for Coupling CO_2 and Epoxides to Cyclic Carbonates: A Rational Design Approach for Organocatalysts

Mannkyu Hong,[†,‡,#] Yoseph Kim,[§,#] Hyejin Kim,[§] Hee Jin Cho,[§]
Mu-Hyun Baik,[*,‡,†] and Youngjo Kim[*,§]

[†]Department of Chemistry, Korea Advanced Institute of Science and Technology (KAIST), Daejeon 34141, Republic of Korea

[‡]Center for Catalytic Hydrocarbon Functionalizations, Institute for Basic Science (IBS), Daejeon 34141, Republic of Korea

[§]Department of Chemistry and BK21+ Program Research Team, Chungbuk National University, Cheongju, Chungbuk 28644, Republic of Korea

ABSTRACT: Novel scorpionate-type organocatalysts capable of effectively coupling carbon dioxide and epoxides under mild conditions to afford cyclic propylene carbonates were developed. Based on a combined experimental and computational study, a precise mechanistic proposal was developed and rational optimization strategies were identified. The epoxide ring-opening, which requires an iodide as a nucleophile, was enhanced by utilizing an immonium functionality that can form an ion pair with iodide, making the ring-opening process intramolecular. The CO_2 activation and cyclic carbonate formation were catalyzed by the concerted action of two hydrogen-bonds originating from two phenolic groups placed at the claw-positions of the scorpionate scaffold. Electronic tuning of the hydrogen-bond donors allowed to identify a new catalyst that can deliver >90% yield for a variety of epoxide substrates within 7 hours at room temperature, a CO_2 pressure of only 10 bar and is highly recyclable.

INTRODUCTION

The steady increase in atmospheric carbon dioxide (CO_2) concentration constitutes a major environmental concern as it is responsible for the global climate change.[1] A sustainable solution for the permanent removal of CO_2 from the atmosphere must entail a chemical technology that converts it to a useful commodity chemical with some economical value. Consequently, CO_2 has attracted significant attention as a source for carbon in various types of chemical reactions.[2,3] Thus, the chemical transformations of CO_2 into value-added commodity chemicals[4,5] such as urea, methanol, cyclic carbonates, poly(propylene carbonate), oxazolidinone and sodium 2-hydroxybenzoate are important reactions to develop. Among these methods, the coupling of CO_2 and epoxides to produce the corresponding cyclic carbonates[6,7] is of particular interest. To date, a wide range of catalytic systems including metal-based catalysts and organocatalysts have been developed for the coupling of CO_2 and epoxides.[3,6–8] However, to complete this reaction, many catalysts require harsh reaction conditions such as high temperatures (> 75 °C), high CO_2 pressures (> 10 bar) and high catalyst loadings (> 5 mol %), which are ultimately associated with additional, indirect CO_2 emissions and limit their value from a technological standpoint. Several metal-based catalytic systems for converting CO_2 to cyclic carbonates at room temperature have been reported.[9] Unlike metal-based catalysts, most of organocatalysts are inexpensive, less toxic, moisture/air stable, easily obtainable and recyclable;[10] however, they are much less reactive than metal-based catalysts. Recently, binary catalytic systems based on polyphenol/nBu$_4X$ (X = Br, I) have been demonstrated to be useful and efficient organocatalysts for the coupling of CO_2 and epoxides in good yields.[11,12] The introduction of multiple hydrogen bond donors onto the phenyl ring allowed for reducing the catalyst loading notably. In addition, ammonium salts[13] and phosphonium salts[14–16] possessing aliphatic[13–15] or phenolic hydroxyl groups[13(a),13(b),16] have been used as bifunctional one-component organocatalysts, but they require elevated reaction temperatures (45–100 °C).[11–17] Organocatalysts capable of performing this C–O reaction at room temperature are rare and the best known catalytic systems are summarized in Table 1.[18–21]

Table 1. Representative organocatalysts for cyclic propylene carbonate synthesis at room temperature

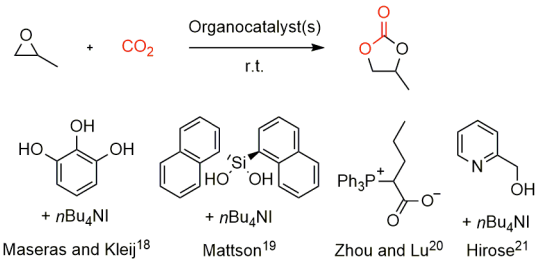

	Maseras and Kleij[18]	Mattson[19]	Zhou and Lu[20]	Hirose[21]
Cat. Loading	5 mol %	10 mol %	2 mol %	8 mol %
Reaction Time	18 h	18 h	4 h	20 h
CO_2 Pressure	10 bar	1 bar	20 bar	1 bar
Yield	63%	74%	91%	86%

On the basis of dramatic catalytic improvements seen when employing multinuclear metal-based complexes which benefit from synergistic and cooperative effects between metal centers linked by bridging ligands,[22] we questioned if similar effects may be available in organocatalysts with dual hydrogen bonds linked by an ammonium salt. Our design consisted of a multifunctional one-component system that employs two alcohol groups capable of hydrogen bonding along with an

ammonium iodide group combined into a single molecule. Extensive calculations of the mechanism based on density functional theory (DFT)[23] was utilized to identify promising catalyst candidates that were subsequently prepared and tested, leading to one of the most effective one-component organocatalysts for the carbonate synthesis to date.

RESULTS AND DISCUSSION

Design & Synthesis of the Multifunctional Catalyst. Hydrogen bond donors are known to activate epoxide ring-opening reactions through coordination to the oxygen of propylene oxide.[14–20] Several carbon dioxide fixation mechanisms involving two hydrogen bond donors have been reported with slightly different pathways.[4,11,14,18,24] Figure 1 summarizes a reasonable consensus mechanism that serves as a starting point for our mechanistic exploration by DFT calculations. The catalytic cycle begins with the two hydrogen bond donors **A** engaging the epoxide substrate to afford **B**, which can be attacked by the nucleophile, for example an anion X^-, traversing the transition state **B-TS** to form the ring-opened alkoxide intermediate **C**. The alkoxide may be stabilized by both hydrogen bond donors, ready to perform a nucleophilic attack on carbon dioxide leading to the C–O bond formation to give the hydrogen-bond stabilized carbonate product complex **D**. Finally, the cyclic carbonate is formed through an internal nucleophilic substitution via the transition state **D-TS**.

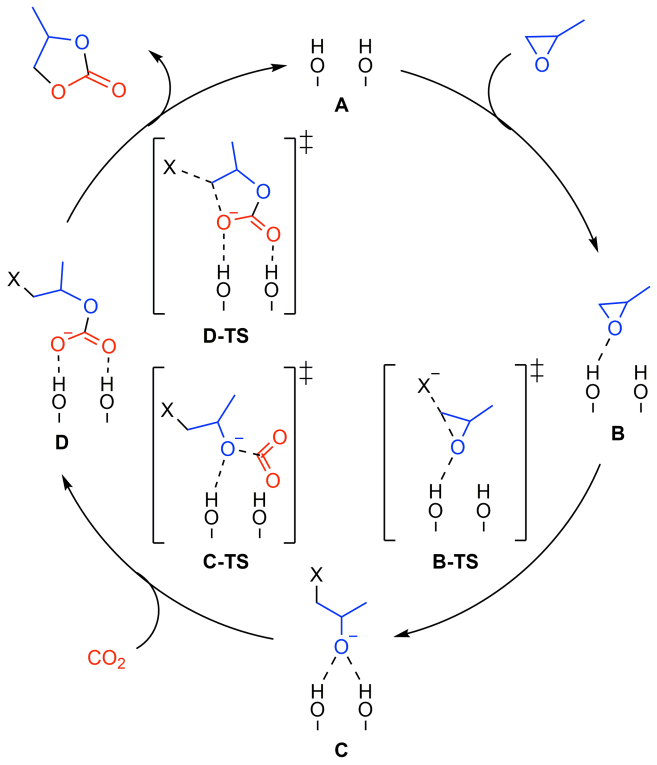

Figure 1. Proposed catalytic cycle for the formation of propylene carbonate by coupling of propylene oxide and CO_2 using two hydrogen bond donors (–OH) and an anion nucleophile (X^-).

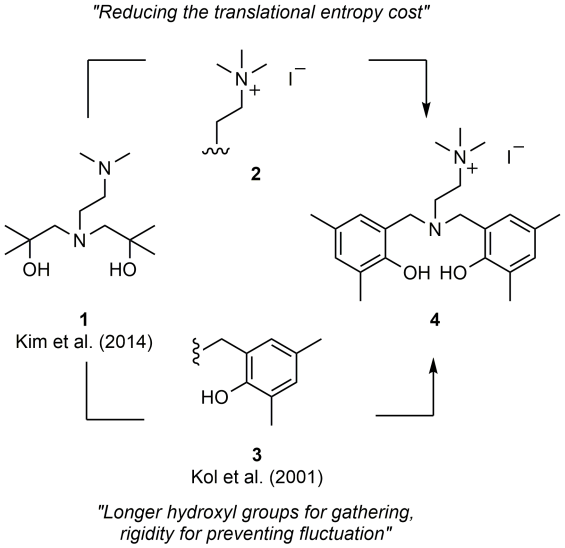

Figure 2. Initial design strategy of the desired catalyst **4**.

Analyzing the proposed mechanism above, we found that the anionic nucleophile and the proximity of the two hydroxyl groups are key features for designing an effective catalyst. Starting with **1** shown in Figure 2,[25] which we had prepared some time ago, we decided to change the terminal amine functionality to a quaternary ammonium/iodide ion pair to afford **2**. The ion pair serves as an intramolecular delivery device for the iodide during the ring-opening attack of the epoxide. This pre-association of the nucleophile to the catalyst via electrostatic attraction is expected to reduce the translational entropy penalty at the ring-opening step when compared to binary systems. By electrostatically associating the iodide to the catalyst and forming an ion pair, the nucleophile is a part of the catalytic system and there is no translational entropy cost during the key step where the iodide must assist the cyclization reaction, as will be shown below. Catalyst **1** showed a very low yield of only 2% (entry 1 in Table 2). When nBu$_4$NI was added as an external iodide source, we observed a notable increase of the yield to 10%. The use of the catalyst **2** incorporating the ammonium/iodide ion pair led to a nearly three-fold increase in yield to 29% (entry 3 in Table 2), which confirms the benefits of the translational entropy cost reduction mentioned above.

Next, we turned our attention to the hydrogen-bonding portion of the catalyst. Using our computer model, we performed a thorough conformer search in an effort to obtain the most relaxed geometry of the catalyst **2**. As illustrated in Figure 3, the preferred geometry displayed the two neopentanol moieties pointing away from each other establishing a distance of nearly 6.5 Å between the two oxygens. This geometry is not ideal for synergistically engaging the substrate propylene oxide. A straightforward optimization strategy is to replace the alkyl fragment by structurally more rigid aryl groups and place the hydroxyl groups where they can more easily engage the central amine functionality in an intramolecular hydrogen bonding interaction, which should allow for a more focused arrangement of these functional moieties during catalytic turnover. Previously, Kol designed ligand **3** and used it to bind zirconium.[26] Inspired by that work, we envisioned that catalyst **4** may be a promising candidate as an organocatalyst for the cyclic carbonate production.

Table 2. Cycloaddition results for catalyst 4 and its derivatives

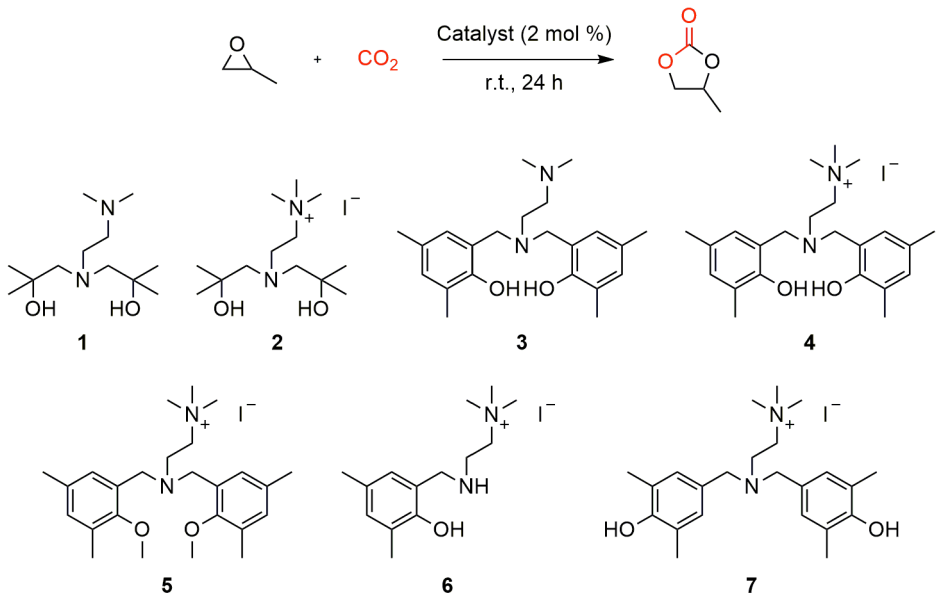

Entry	Catalyst	CO_2 Pressure (Bar)	Yield (%)
1	**1**	10	2
2	**1** + nBu$_4$NI	10	10
3	**2**	10	29
4	**3**	10	7
5	**3** + nBu$_4$NI	10	13
6	**4**	10	85
7	**5**	10	11
8	**6**	10	30
9	**7**	10	43
10	**3** + nBu$_4$NI	5	6
11	**4**	5	69
12	**5**	5	6
13	**6**	5	17
14	**4**	1	42

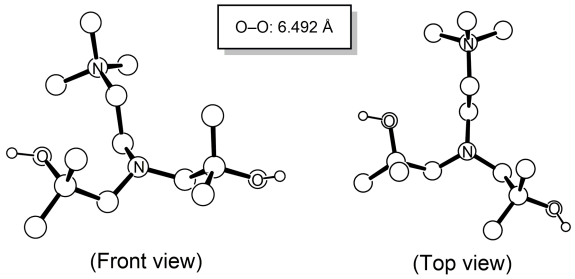

Figure 3. Energetically lowest structure of **2**. Iodide and non-essential hydrogens are not shown for clarity.

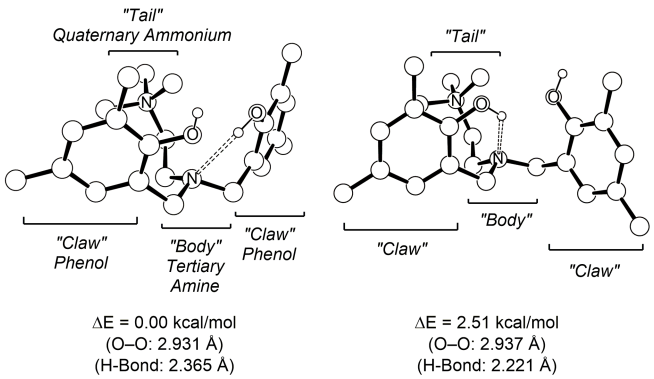

Figure 4. Two energetically lowest structures of catalyst **4**. Iodide and non-essential hydrogens are not shown for clarity.

Catalyst **4** was examined carefully by an extensive conformer search using computationally efficient molecular mechanics models followed by DFT calculations. Two of the lowest energy structures that are most important for the catalytic activity of the catalyst are shown in Figure 4 and they exhibit the characteristics of scorpionate ligands. As designed, the phenolic hydroxyl groups form weak hydrogen bonds with the tertiary amine and with each other resulting in a O–O distance of only ~2.93 Å. To confirm the hydrogen bond accepting role of the tertiary amine, we replaced the nitrogen atom by a (C–H) fragment and used the identical computational protocol to obtain the lowest energy structures. We were unable to find any structures that showed the directional bias for the hydrogen bond donors that we wished to engineer (Table S3). To test our computer-aided design, we prepared catalyst **4** by adding 1.7 g (12 mmol) methyl iodide to a 25 mL solution of 6,6'−(((2−(dimethylamino)ethyl)azanediyl)bis(methylene))bis(2,4−dimethylphenol) (**3**) (1.1 g, 3.0 mmol), as summarized in Scheme 1. All volatiles were removed at reduced pressure and the obtained crude solid was washed with diethyl ether (3 × 40 mL). Then they were removed *in vacuo* to give the desired product **4** (1.4 g, 92 %) as yellow solid.

Scheme 1. Synthesis of catalyst 4 from precursor 3

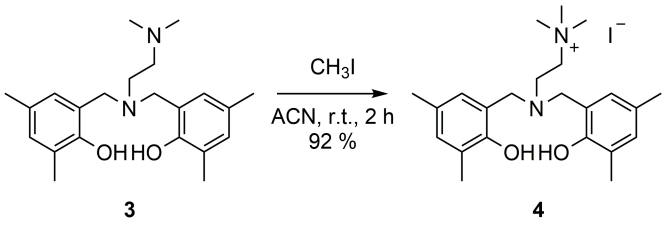

3 **4**

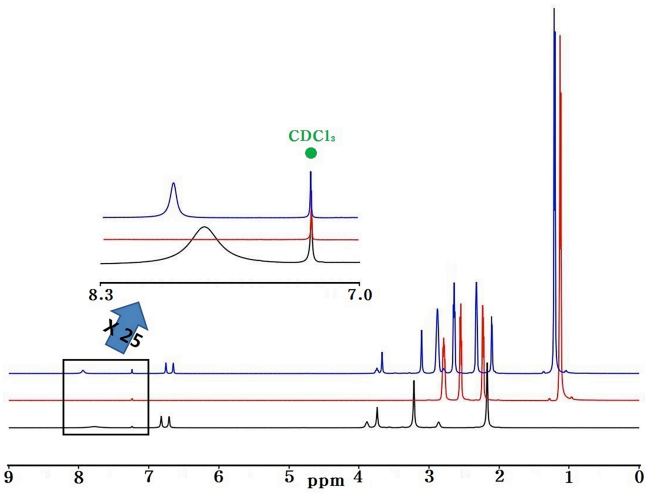

Figure 5. ^{1}H-NMR spectra corresponding to the analyses of catalyst **4** (Black line), propylene oxide (Red line), and a mixture of **4** and propylene oxide (Blue line).

The scorpionate structure of compound **4** discussed above was confirmed by single-crystal X-ray diffraction analysis (Table S9). The hydrogen bond between the tertiary amine and one of the phenols persists in solution, as indicated by a broadened ^{1}H-NMR peak at 7.78~7.49 ppm shown in Figure 5. The internal hydrogen bonds not only keep the two hydrogen bond donors aligned but also create a binding cavity for the substrate. To further test the design strategy, various analogues of **1** and **4** were prepared, as summarized in Table 2. The derivative **5** contains no hydroxyl groups, and have methoxy substituents, instead. Catalyst **6** offers only half of catalyst **4** and should allow for estimating the effect of two hydrogen-bond donors. And finally, in catalyst **7** the hydroxyl groups were moved to the *para*-position. All these derivatives should be less effective catalysis than **4**.

The catalytic activities of these catalyst candidates under mild conditions using 2 mol % catalyst loading in 24 hours reaction time are summarized in Table 2. Catalyst **3** gave only 7% yield demonstrating that closely placed diphenol cores alone are not sufficient. The binary catalytic system of **3** with *n*Bu_4NI as a nucleophile showed a slightly increased but still poor yield of 13% (entry 5). Catalyst **4** with two phenol groups combined with the ammonium on the tail, on the other hand, gave outstanding yield of 85% under the same reaction conditions (entry 6), confirming our design principles described above. Expectedly, the catalysis does not work well without the hydroxyl moieties, and we found a dramatic loss of catalytic activity to yield only 11% product when **5** was employed. Catalyst **6** also afforded a lower yield of 30%, highlighting the importance of having two hydrogen-bond donors in catalyst **4**.[12] Catalyst **7** was surprisingly active, but still showed lower yield of 43%. The results support our proposed design principle.

To investigate the dependence of the catalytic activity on CO_2 pressure, the CO_2 pressure was reduced to 5 bar and the results are shown in the entries 10–13 in Table 2. The product yield dropped consistently for all systems by ~50%, but catalyst **4** still showed a respectable 69% yield. Even when the CO_2 pressure was further lowered to only 1 bar, we were able to observe 42% conversion with **4**. Thus, this new, rationally designed scorpionate system offers significant improvements over previous organocatalysts, as it operates not only at room temperature and with a low catalyst loading of 2 mol %, but also under solvent-

free conditions. Increasing the temperature to 50 °C, reaction time could be reduced to 12 h. To further validate the mechanism, a series of ^{1}H-NMR investigations of **4**, propylene oxide, and a mixture of **4** and propylene oxide in $CDCl_3$ (0.5 mL) was conducted and we found good evidence for the reaction proceeding as illustrated for A → C in Figure 1. As shown in Figure 5, the region between 7.0 and 8.3 ppm displays a downfield shifted phenolic OH signal of **4** from 7.78 to 7.94 ppm upon replacement of iodide to epoxide coordination at the diphenol core. The change induced in the electronic environment of propylene epoxide by the interaction with the hydrogen bond donors was also observed. The overall downfield shift of four proton peaks from propylene oxide supports the activation of propylene oxide by coordination to the two phenol groups.

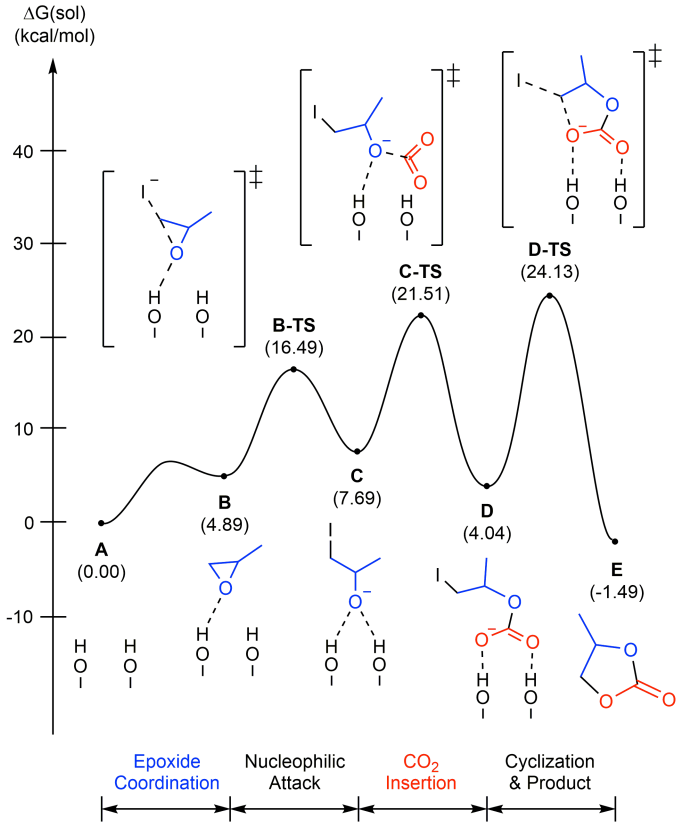

Figure 6. Computed energy profile for propylene carbonate formation with catalyst **4**.

Mechanism. To fully understand the catalytic reaction and identify additional strategies for optimizing the catalyst, the mechanism of the carbonate forming reaction using catalyst **4** was calculated and the computed reaction energy profile is illustrated in Figure 6. The catalytic cycle follows the general pattern outlined above. As designed, the nucleophilic attack leading to the ring-opening of the epoxide, associated with the transition state **B-TS** is relatively easy with a barrier of only 16.5 kcal/mol and the nucleophilic attack towards the CO_2 substrate is also reasonable at a barrier of 21.5 kcal/mol traversing the transition state **C-TS**. Interestingly, all steps leading up to the final cyclization and release of the product are slightly uphill energetically and the barrier for the cyclization is the highest of all step barriers. Thus, we do not expect any of the intermediates to accumulate to constitute a classical resting state of the catalysis. The most difficult step is the cyclization with an overall barrier of 24.1 kcal/mol. Figure 7 shows the computed structure of the transition state **D-TS**, where the carbonate oxygen

attacks the carbon center carrying the iodide in this SN2-type transition state. The computed structure shows clearly how the two hydrogen-bonds stabilize the carboxylate moiety, with the calculated O–HO distance being 1.73 and 1.92 Å, respectively. Interestingly, the elimination of iodide is supported by the cationic ammonium moiety and we found the I–N distance to be 4.53 Å. To quantify the synergistic effect of the two hydrogen-bond donors, we calculated the barrier with one hydroxide group rotated away from the carbonate substrate and found the new putative transition state to be 4.9 kcal/mol higher in energy at 29.0 kcal/mol. Thus, our calculations suggest that the second hydrogen bond gives rise to a 3-4 fold acceleration.

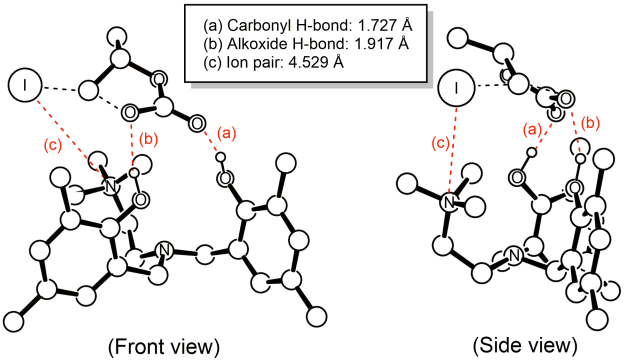

Figure 7. Description of the highest barrier (**D-TS**) and the three possible non-covalent interactions that influences the barrier. Non-essential hydrogens are not shown for clarity.

Catalyst Optimization. With the mechanism understood and the exact role of the different components of the scorpionate scaffold identified, we questioned if the yield of 85% can be further improved. First, several control experiments were carried out to challenge our proposed mechanism. Based on the mechanistic insights we obtained, we do not expect any benefits from changing the functional group at the ammonium tail to anything larger than the methyl groups, as the ion pairing ability should be lessoned by any sterically demanding functionalities. Similarly, iodide should be an ideal nucleophile among the halogenide series, as the carbon-iodine bond should be easiest to break at the **D-TS** state and iodide should be the best leaving group. In good agreement with these expectations, we were able to confirm that modifications of the ammonium tail of the scorpionate led to significant loss of catalytic performance, as enumerated in Table 3. Catalysts **8** and **9** afforded 41 and 16% yield, respectively. Changing the nucleophile to bromide, chloride or nitrate had devastating effects on the catalysis with yields dropping to single digit % values.

Table 3. Tail modification results of the parent catalyst 4

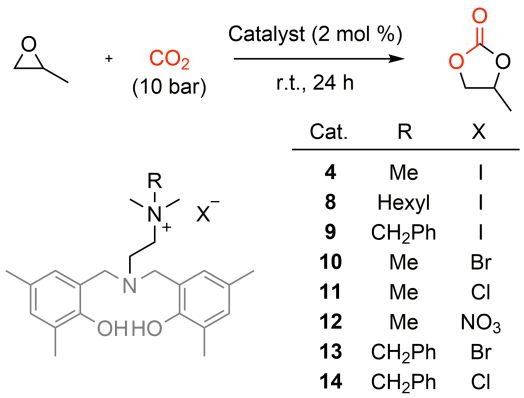

Cat.	R	X
4	Me	I
8	Hexyl	I
9	CH_2Ph	I
10	Me	Br
11	Me	Cl
12	Me	NO_3
13	CH_2Ph	Br
14	CH_2Ph	Cl

Entry	Catalyst	Yield (%)
1	**4**	85
2	**8**	41
3	**9**	16
4	**10**	11
5	**11**	3
6	**12**	3
7	**13**	8
8	**14**	5

Next, we turned our attention to the claw portion of the scorpionate and explored several strategies for electronically modifying the phenyl moiety. Unsurprisingly, the *para*-position to the hydroxyl functionality was found to be a particularly promising substitution site. Fundamentally, two scenarios can be imagined: (*i*) Installing electron-withdrawing groups will increase the pK_a of the hydroxyl-proton and make it a more potent hydrogen-bond donor, thus substrate binding will be tighter, which may be an advantage for catalytic activity. (*ii*) Electron-donating groups, on the other hand, will weaken the hydrogen-bonds, which will destabilize the intermediates, but may prove to enhance the rate of the reaction if hydrogen-bond breaking is involved in the key transition state. Previously, D'Elia reported hydrogen-bond mediated organocatalysts where the CO_2 conversion efficiency changes depending on different moieties of an ascorbic acid.[24(c)] In our case, we already identified that the hydrogen-bond between the oxo moiety and the claw of the scorpionate must be cleaved at the key transition state **D-TS**. Thus, our expectation is that the weakening the hydrogen-bond should lower the cyclization barrier. And this expectation is fully confirmed by our DFT-calculations, as shown in Figure 8 (see Figure S1 for full profile). Note that the reference catalyst shown in Figure 8 is **4'**, which is minimally different from **4**, as we removed the methyl group at the *ortho*-position of the hydroxyl. We did not find any meaningful difference between **4** and **4'** in our computer simulations. Because the electron-withdrawing nitro group strengthens the hydrogen-bonding interaction between the substrate and the claw portion of the catalyst, the intermediates are generally lower in energy, and the step barriers to reach transition states that require the rearrangement of hydrogen-bonds are generally higher. The electron-donating NMe_2 moiety, shown in red in Figure 8, has the opposite effect where the energy gap between the intermediates and the following transition-states are smaller, leading to a predicted barrier of 21.0 kcal/mol for the cyclization step, which is nearly 4 kcal/mol lower in energy than what was found for catalyst **4**. As illustrated in Figure 8b, the hydrogen bond lengthens by ~0.04 Å upon reaching **D-TS** and the predicted barrier

decreases to 21.0 kcal/mol when R=NMe_2, whereas 23.3 kcal/mol is found for R=NO_2. This result is in good agreement with our conceptual proposal that the weakening of the hydrogen bond strength should lower the energy of the **D-TS** transition state.

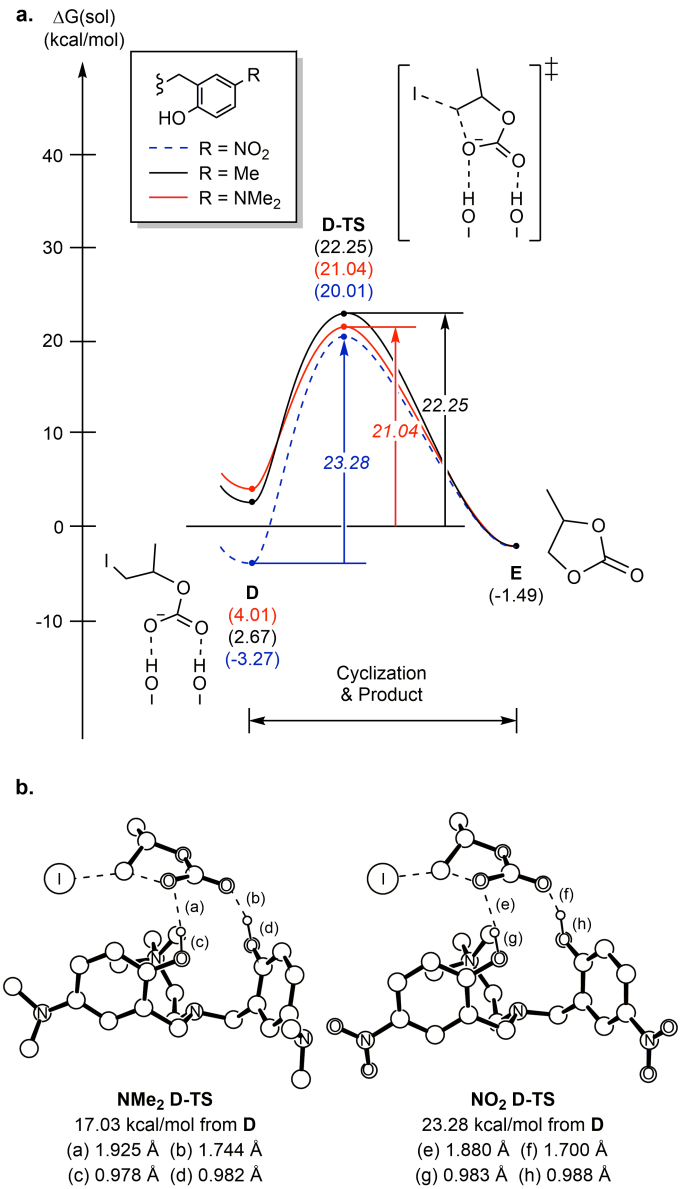

Figure 8. Comparison of the energies and structures of cyclization step catalyzed by **4'** and derivatives. Non-essential hydrogens are not shown for clarity.

To test this computational prediction, we prepared a series of new catalysts with substituents that have increasing electron-donating abilities spanning Hammett σ_p values from 0.78 for NO_2 to –0.83 for NMe_2[27] as shown in Table 4. Their catalytic performance was assessed with the reaction time shortened to 14 hours for convenience. As predicted, the substituents NO_2, Br and H show notable degradation of catalytic activity with yields being 5, 19 and 46%, respectively. Electron-donating groups generally show higher reactivity and catalyst **18** bearing a ^{t}Bu group displayed a 99% yield (entry 5) and even at 10 h

we were able to obtain 85% yield (entry 9). The catalysts with OMe and NMe_2 functionalities in the *para*-position showed a somewhat disappointing 28 and 70% yield, respectively. A closer analysis revealed, however, that these catalysts were not very soluble in neat propylene oxide. Thus, we repeated the experiments after adding 0.3 mL of DMSO, which allowed the catalysts to be fully dissolved and the yields were much higher, although we shortened the reaction time further to 8 and in the last case to 7 hours: Catalysts **18**, **19** and **20** gave propylene carbonate products in 68, 73 and 98% yield, respectively. Therefore, **18** and **20** are remarkably efficient and among the most effective hydrogen bond mediated one-component organocatalysts for propylene carbonate synthesis discovered to date.

Table 4. Claw modification results of the parent catalyst 4'

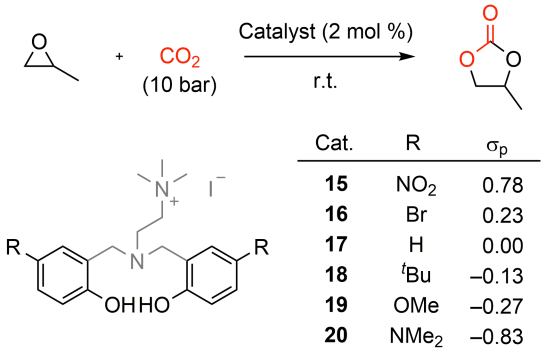

Cat.	R	σ_p
15	NO_2	0.78
16	Br	0.23
17	H	0.00
18	^{t}Bu	–0.13
19	OMe	–0.27
20	NMe_2	–0.83

Entry	Catalyst	Time (h)	Yield (%)
1	**4**	24	85
2	**15**	14	5
3	**16**	14	19
4	**17**	14	46
5	**18**	14	99
6	**19**	14	28
7	**20**	14	70
8	**18**	10	85
9[a]	**15**	8	4
10[a]	**16**	8	12
11[a]	**18**	8	68
12[a]	**19**	8	73
13[a]	**20**	7	98

[a]Reaction conditions: Propylene oxide (10 mmol), Organocatalyst (0.20 mmol), DMSO (0.3 mL)

Table 5. Substrate scope

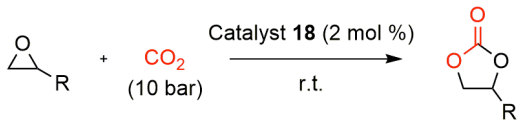

Entry	R	Time (h)	Yield (%)
1	Me	12	99
2	CH_2Cl	6	90
3	CH_2OH	6	96
4	CH_2OMe	12	96
5	CH_2O^tBu	12	94
6	CH_2OPh	12	93

From technical perspective, the requirement of having to add a cosolvent to solubilize the catalyst is a decisive disadvantage. For that reason, we continued our studies using catalyst **18**, although it is slightly less active than **20** and requires a slightly longer reaction time. The substrate scope was examined and the results are shown in Table 5. Epoxides containing various functional groups could be employed to obtain the corresponding products in good to high yields (90–99% yield, entries 2–6) at room temperature. The variation in substrate did not reduce catalytic efficiency, and epichlorohydrin (entry 2) and glycidol (entry 3) were converted within a shorter reaction time (6 h) than other epoxides.

Table 6. Recycling of catalyst 18

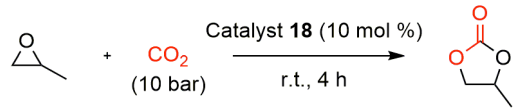

Cycles	Yield (%)
1	99
2	98
3	99
4	97
5	98

Next, we investigated the effects of reaction temperature (25–125 °C) and pressure (0.5–3 MPa) (Table S10). The results show that catalytic efficiency is proportional to reaction temperature, whereas reaction pressure was not an important factor. Finally, we tested how recyclable the catalyst is, as the excellent stability often observed for organocatalysts and the resulting recyclability is an important advantage over other competing processes. The recyclability of **18** was tested using accelerated test conditions (25 °C, $p(CO_2)$ = 10 bar, time = 4 h, catalyst loading = 10 mol %). At the end of each reaction, the catalyst was precipitated and reused in the next run with at same conditions. As summarized in Table 6, the activity of the catalyst remained high (> 97% conversion) over five cycles. Our multifunctional scorpionate organocatalyst **18** possesses not only high reactivity but also excellent reusability.

CONCLUSION

In conclusion, we developed one of the most effective one-component organocatalyst to date for the generation of cyclic propylene carbonate by coupling propylene oxide and CO_2 at room temperature. The catalyst was rationally designed in a combined experimental and computational effort based on a clear conceptual vision. First, we made use of an ammonium group to bind a nucleophilic iodide as an ion pair, thus incorporating the nucleophile that is needed for the epoxide ring-opening into the catalyst. This effectively reduces the translational entropy penalty that must be paid if the ring-opening is achieved by an intermolecular reaction. Second, we placed two phenolic hydrogen-bond donors that are tethered by a tertiary amine moiety, which serves a temporary hydrogen-bond acceptor to keep the two phenolic groups in close proximity. Lastly, we explored the decoration of the aryl arms of this scorpionate type catalyst at the *para*-position to the hydroxyl groups with electron-donating groups to weaken to hydrogen-bonds. This weakening of the hydrogen-bonds allowed for the cyclization step to be easier, leading to a notable increase in overall reactivity. The optimized catalyst was highly effective in forming cyclic carbonates with a wide range of different substrate under ambient conditions. This new catalyst is easy to make and it was found to be fully recyclable over five cycles without any loss of efficiency. This work demonstrates the power of combining the deep mechanistic insight that can be gained by sophisticated computer models with targeted experimental explorations of novel catalyst scaffolds.

EXPERIMENTAL SECTION

General Experimental Methods. All manipulations were performed under an atmosphere of dinitrogen by using standard Schlenk−type glassware with a dual manifold Schlenk line.[28,29] Dinitrogen was deoxygenated using an activated Cu catalyst and was dried with drierite.[30] All chemicals were purchased from Aldrich and used as supplied unless otherwise indicated. Carbon dioxide (99.999%) was used as received without further purification. All solvents such as toluene, diethyl ether, and *n*-hexane, were dried by distillation from sodium diphenylketyl under dinitrogen and were stored over 3 Å activated molecular sieves. ^{1}H and ^{13}C NMR spectra were recorded at ambient temperature on a Bruker DPX−400 MHz and 500 MHz NMR spectrometer using standard parameters. All chemical shifts are reported in δ units referenced to the residual D_2O (δ 4.79 for ^{1}H NMR), $CDCl_3$ (δ 7.24 for ^{1}H NMR; δ 77.00 for ^{13}C NMR), DMSO-d_6 (δ 2.50 for ^{1}H NMR; δ 39.52 for ^{13}C NMR), or CD_3CN (δ 1.94 for ^{1}H NMR; δ 61.50, 118.26 for ^{13}C NMR). High-resolution mass spectra (HRMS) were acquired on a high resolution Q-TOF mass spectrometer (ionization mode : ESI).

Representative Procedures for the Coupling Reaction of Epoxide and CO_2. The coupling reaction of CO_2 to epoxide was carried out by charging a stirring bar, epoxide (10 mmol), and catalyst (0.20 mmol) into a stainless steel pressure reactor (10 mL inner volume). Then, CO_2 was charged and the pressure was adjusted to a desired pressure at appropriate temperature. After given reaction hours, the pressure reactor was cooled to ambient temperature, and the excess CO_2 was vented. All volatiles were removed under vacuo and the precipitated catalyst was removed by filtration. The purity of cyclic carbonates obtained was checked by ^{1}H NMR spectroscopy.

Synthesis of Known Compounds. Compounds 1,1'−((2−(dimethylamino)ethyl)azanediyl)bis(2−methylpropan−2−ol) (**1**),[25] 6,6'−(((2−(dimethylamino)ethyl)azanediyl)bis(methylene))bis(2,4−dimethylphenol) (**3**),[26] 2−(((2−(dimethylamino)ethyl)imino)methyl−4,6−dimethylphenol,[31]

4,4'−(((2−(dimethylamino)ethyl)azanediyl)bis(methylene))bis(2,6−dimethylphenol),[32]
2,2'−(((2−(dimethylamino)ethyl)azanediyl)bis(methylene))bis(4−nitrophenol),[33]
2,2'−(((2−(dimethylamino)ethyl)azanediyl)bis(methylene))diphenol,[34] and
2,2'−(((2−(dimethylamino)ethyl)azanediyl)bis(methylene))bis(4−methoxyphenol)[35] were prepared by previously published procedures.

Synthesis of 2-(bis(2-hydroxy-2-methylpropyl)amino)-*N*,*N*,*N*-trimethylethan-1-aminium iodide (2). To a solution of **1** (0.69 g, 3.0 mmol) in MeCN (25 mL) at 50 °C was added methyl iodide (1.7 g, 12 mmol), and the mixture was refluxed. After 12 h, the reaction mixture was cooled to room temperature and all volatiles were removed at reduced pressure. The obtained crude solids were washed with diethyl ether (3 × 40 mL). All volatiles were then removed *in vacuo* to give the desired product **2** (1.06 g, 95 %) as a colorless solid; mp 146.4−148.2 °C; ^{1}H NMR (D_2O, 400.13 MHz): δ 3.53 (t, 2H, J = 8.4 Hz, −CH_2NMe$_3$), 3.18 (t, 2H, J = 5.0 Hz, −NCH_2CH$_2$NMe$_3$), 3.15 (s, 9H, −NMe_3), 2.66 (s, 4H, −NCH_2CMe$_2$OH), 1.21 (s, 12H, CMe_2). ^{13}C NMR (D_2O, 100.61 MHz): δ 72.6, 67.3, 63.2, 53.4 (t, J = 4.9 Hz), 51.0, 26.5. HRMS: calcd. for $C_{13}H_{31}N_2O_2$ [M – I$^-$]$^+$ = 247.2380; found 247.2380.

Synthesis of 2−(bis(2−hydroxy−3,5−dimethylbenzyl)amino−*N*,*N*,*N*−trimethylethan-1-aminium iodide (4). The desired product **4** (1.4 g, 92 %) as a yellow solid was prepared by reacting compound **3** (1.1 g, 3.0 mmol) with methyl iodide (1.7 g, 12 mmol) in a manner analogous to the procedure for **2**. A yellow crystal suitable for single X-ray analysis was obtained from NMR cell; mp 120.8−123.4 °C; ^{1}H NMR ($CDCl_3$, 500.13 MHz): δ 7.68 (s, 2H, −O*H*), 6.87 (s, 2H, Ar−*H*), 6.74 (s, 2H, Ar−*H*), 3.90 (t, 2H, J = 6.6 Hz, −CH_2NMe$_3$), 3.79 (s, 4H, ArCH_2N−), 3.22 (s, 9H, −NMe_3), 2.87 (t, 2H, J = 6.6 Hz, −NCH_2CH$_2$NMe$_3$), 2.22 (s, 6H, ArCH_3), 2.20 (s, 6H, ArCH_3). ^{13}C NMR ($CDCl_3$, 100.61 MHz): δ 151.7, 131.6, 129.1, 128.9, 124.8, 121.0, 64.4, 55.9, 54.0, 45.2, 20.4, 16.6. HRMS: calcd. for $C_{23}H_{35}N_2O_2$ [M – I$^-$]$^+$ = 371.2699; found 371.2700.

Synthesis of 2−(bis(2−methoxy−3,5−dimethylbenzyl)amino)−*N*,*N*,*N*−trimethylethan−1−aminium iodide (5). To a solution of NaH (0.43 g, 18 mmol) in THF (25 mL) at room temperature was dropwise added compound **3** (1.1 g, 3.0 mmol) in THF (25 mL), and the mixture was stirred for 3 h. To the reaction mixture was added methyl iodide (4.3 g, 30 mmol), and the mixture was refluxed for overnight. The reaction mixture was cooled to room temperature and added distilled water (40 mL). The reaction mixture was extracted with dichloromethane and the yellow phase was dried with $MgSO_4$. And then the solution was filtered and evaporated under reduced pressure with a rotary evaporator to give the desired product **5** (0.57 g, 36 %) as a yellow solid; mp 145.6−148.3 °C; ^{1}H NMR ($CDCl_3$, 400.13 MHz): δ 6.90 (s, 4H, Ar−*H*), 3.60 (s, 6H, −OCH_3), 3.57 (s, 6H, ArCH_2N− and −CH_2NMe$_3$), 3.13 (s, 9H, −NMe_3), 2.83 (s, 2H, −NCH_2CH$_2$NMe$_3$), 2.24 (s, 6H, ArCH_3), 2.22 (s, 6H, ArCH_3). ^{13}C NMR ($CDCl_3$, 100.62 MHz): δ 155.1, 133.4, 131.7, 131.0, 129.9, 129.6, 63.6, 60.9, 54.1, 53.6, 47.2, 20.8, 16.1. HRMS: calcd. for $C_{25}H_{39}N_2O_2$ [M – I$^-$]$^+$ = 399.3012; found 399.3012.

Synthesis of 2−((2−hydroxy−3,5−dimethylbenzyl)amino)−*N*,*N*,*N*−trimethylethan−1−aminium iodide (6). To a solution of 2−(((2−(dimethylamino)ethyl)imino)methyl−4,6−dimethylphenol (0.66 g, 3.0 mmol) in MeCN (25 mL) at 50 °C was added methyl iodide (0.48 g, 3.3 mmol), and the mixture was refluxed. After 12 h, the reaction mixture was cooled to room temperature and all volatiles were removed at reduced pressure. The obtained crude solids were washed with diethyl ether (3 × 40 mL). All volatiles were then removed *in vacuo* to give 2−((2−hydroxy−3,5−dimethylbenzylidene)amino−*N,N,N*−trimethylethan−1-aminium iodide (0.96 g, 88 %) as a yellow solid; mp 134.6−135.8 °C; ^{1}H NMR (DMSO-d_6, 400.13 MHz): δ 12.9 (s, 1H, O*H*), 8.60 (s, 1H, ArC*H*=N), 7.08 (s, 2H, Ar−*H*),

4.06 (s, 2H, −CH_2NMe$_3$), 3.71 (t, 2H, J = 6.2 Hz, −NCH_2CH$_2$NMe$_3$), 3.14 (s, 9H, −NMe_3), 2.22 (s, 3H, ArCH_3), 2.14 (s, 3H, ArCH_3). ^{13}C NMR (DMSO-d_6, 125.76 MHz): δ 168.6, 156.1, 134.5, 129.4, 126.9, 124.7, 117.4, 65.6, 52.9, 51.8, 19.9, 15.1. HRMS: calcd. for $C_{14}H_{23}N_2O$ [M – I$^-$]$^+$ = 235.1811; found 235.1805. To a solution of 2−((2−hydroxy−3,5-dimethylbenzylidene)amino-*N,N,N*−trimethylethan−1−aminium iodide (0.72 g, 2.0 mmol) in methanol (25 mL) at 0 ^{o}C was slowly added $NaBH_4$ (0.38 g, 10 mmol), and the mixture was stirred for 3 h at room temperature. To the reaction mixture was added distilled water (40 mL), and the mixture was stirred for 3 h at room temperature. The reaction mixture was extracted with dichloromethane, and then the yellow organic phase was dried with $MgSO_4$. The solution was filtered and evaporated under reduced pressure to give the desired product **6** (0.58 g, 80 %) as a yellow solid; mp 139.6−141.3 ^{o}C; ^{1}H NMR (DMSO-d_6, 400.15 MHz): δ 6.79 (s, 1H, Ar−*H*), 6.72 (s, 1H, Ar−*H*), 3.79 (s, 2H, ArCH_2−), 3.46 (t, 2H, J = 6.4 Hz, −CH_2NMe$_3$), 3.10 (s, 9H, −NMe_3), 2.94 (t, 2H, J = 6.4 Hz, −NCH_2CH$_2$NMe$_3$), 2.14 (s, 3H, ArCH_3), 2.08 (s, 3H, ArCH_3). ^{13}C NMR (DMSO-d_6, 100.63 MHz): δ 152.7, 129.9, 126.8, 126.7, 123.8, 123.0, 63.9, 52.7, 50.5, 41.6, 20.1, 15.8. HRMS: calcd. for $C_{14}H_{25}N_2O$ [M – I$^-$]$^+$ = 237.1967; found 237.1961.

Synthesis of 2−(bis(4−hydroxy−3,5−dimethylbenzyl)amino)−*N,N,N*−trimethylethan−1−aminium iodide (7). The desired product **7** (1.3 g, 87 %) as a yellow solid was prepared by reacting compound 4,4'−(((2−(dimethylamino)ethyl)azanediyl)bis(methylene))bis(2,6−dimethylphenol) (1.06 g, 3.0 mmol) with methyl iodide (1.7 g, 12 mmol) in a manner analogous to the procedure for **2**; mp 148.3−151.9 ^{o}C; ^{1}H NMR (DMSO-d_6, 400.13 MHz): δ 8.82 (s, 2H, −O*H*), 7.19 (s, 4H, Ar−*H*), 4.41 (m, 4H, J_1 = 25 Hz, J_2 = 24 Hz, J_3 = 13 Hz, ArCH_2−), 3.99 (m, 2H, −CH_2NMe$_3$), 3.54 (m, 2H, −NCH_2CH$_2$NMe$_3$), 3.33 (s, 9H, −NMe_3), 2.19 (s, 12H, ArCH_3). ^{13}C NMR (DMSO-d_6, 100.61 MHz): δ 149.4, 134.7, 129.8, 123.2, 62.1, 54.2, 42.2, 26.1, 23.0. HRMS: calcd. for $C_{23}H_{35}N_2O_2$ [M – I$^-$]$^+$ =371.2693; found 371.2693.

Synthesis of *N*−(2−(bis(2−hydroxy−3,5−dimethylbenzyl)amino)ethyl)−*N,N*−dimethylhexan−1−aminium iodide (8). The desired product **8** (1.5 g, 85 %) as a yellow solid was prepared by reacting **3** (1.1 g, 3.0 mmol) with 1-iodohexane (2.5 g, 12 mmol) in a manner analogous to the procedure for **2**; mp 137.8−139.7 ^{o}C; ^{1}H NMR ($CDCl_3$, 500.13 MHz): δ 7.76 (s, 2H, −O*H*), 6.87 (s, 2H, Ar−*H*), 6.75 (s, 2H, Ar−*H*), 3.83 (s, 4H, ArCH_2N−), 3.73 (t, 2H, J = 7.0 Hz, −NCH$_2$CH_2NMe$_2$(CH$_2$)$_5$CH$_3$), 3.17 (s, 6H, −NCH$_2$CH$_2$NMe_2(CH$_2$)$_5$CH$_3$), 2.83 (t, 2H, J = 7.0 Hz, −NCH_2CH$_2$NMe$_2$(CH$_2$)$_5$CH$_3$), 2.24 (s, 6H, ArCH_3), 2.20 (s, 6H, ArCH_3), 1.19 (m, 10H, −NMe$_2$CH_2CH_2CH_2CH_2CH$_3$), 0.85 (t, 3H, J = 8.5 Hz, −NMe$_2$CH$_2$CH$_2$CH$_2$CH$_2$CH$_2$CH_3). ^{13}C NMR ($CDCl_3$, 125.76 MHz): δ 151.8, 131.6, 129.1, 128.8, 124.9, 121.1, 64.5, 61.1, 56.1, 52.0, 44.6, 31.0, 25.6, 22.4 (2C), 20.4, 16.6, 13.8. HRMS: calcd. for $C_{28}H_{45}N_2O_2$ [M – I$^-$]$^+$ = 441.3481; found 441.3475.

Synthesis of *N*−benzyl−2−(bis(2−hydroxy−3,5−dimethylbenzyl)amino)−*N,N*−dimethylethan−1−aminium iodide (9). The desired product **9** (1.5 g, 85 %) a colorless solid was prepared by reacting **3** (1.1 g, 3.0 mmol) with benzyl iodide (1.3 g, 6.0 mmol) in a manner analogous to the procedure for **2**; mp 157.8−160.3 ^{o}C; ^{1}H NMR ($CDCl_3$, 400.13 MHz): δ 7.64 (s, 2H, −O*H*), 7.39 (m, 5H, −NMe$_2$CH$_2$*Ph*), 6.86 (s, 2H, Ar−*H*), 6.73 (s, 2H, Ar−*H*), 4.74 (s, 4H, −NMe$_2$CH_2Ph), 3.83 (t, 2H, J = 6.6 Hz, −CH_2NCH$_2$Ph), 3.76 (s, 4H, ArCH$_2$N−), 3.01 (s, 6H, −NMe_2CH$_2$Ph), 2.93 (t, 2H, J = 6.6 Hz, −NCH_2CH$_2$NCH$_2$Ph), 2.21 (d, 12H, J = 8.2 Hz, ArCH_3). ^{13}C NMR ($CDCl_3$, 100.61 MHz): δ 151.7, 133.1, 131.5, 130.8, 129.2, 129.0, 128.8, 126.6, 124.9, 121.4, 67.7, 61.4, 56.0, 49.9, 45.3, 20.4, 16.6. HRMS: calcd. for $C_{29}H_{39}N_2O_2$ [M – I$^-$]$^+$ = 447.3012; found 447.3006.

Synthesis of 2−(bis(2−hydroxy−3,5−dimethylbenzyl)amino−*N,N,N*−trimethylethan-1-aminium bromide (10). To a solution of compound **4** (0.99 g, 2.0 mmol) in THF (25 mL) at room temperature was added silver bromide (0.41 g, 2.2

mmol), and the mixture was stirred for 3 h. The reaction mixture was then filtered through Celite. All volatiles were removed *in vacuo*, and the residue was washed with diethyl ether. The desired product **10** (0.71 g, 79 %) as a beige powder was obtained after vacuum drying; mp 166.4−168.4 °C; ^{1}H NMR (DMSO-d_6, 400.13 MHz): δ 8.95 (s, 2H, −O*H*), 6.84 (s, 2H, Ar−*H*), 6.81 (s, 2H, Ar−*H*), 3.68 (s, 4H, PhCH_2N−), 3.58 (t, 2H, J = 7.6 Hz, −CH_2NMe$_3$), 2.98 (s, 9H, −N*Me*$_3$), 2.82 (t, 2H, J = 7.6 Hz, −CH_2CH$_2$NMe$_3$), 2.16 (s, 6H, ArCH_3), 2.12 (s, 6H, ArCH_3). ^{13}C NMR (DMSO-d_6, 100.61 MHz): δ 152.0, 130.7, 128.3, 127.4, 124.2, 122.3, 60.6, 53.9, 52.4, 44.7, 20.1, 16.2. HRMS: calcd. for $C_{23}H_{35}N_2O_2$ [M – Br$^-$]$^+$ = 371.2699; found 371.2699.

Synthesis of 2−(bis(2−hydroxy−3,5−dimethylbenzyl)amino−*N*,*N*,*N*−trimethylethan-1-aminium chloride (11). The desired product **11** (0.66 g, 81 %) as a beige powder was prepared by reacting compound **4** (0.99 g, 2.0 mmol) with silver chloride (0.32 g, 2.2 mmol) in a manner analogous to the procedure for compound **10**; mp 148.6−150.4 °C; ^{1}H NMR (DMSO-d_6, 400.13 MHz): δ 8.99 (s, 2H, −O*H*), 6.83 (s, 2H, Ar−*H*), 6.82 (s, 2H, Ar−*H*), 3.69 (s, 4H, PhCH_2N−), 3.62 (br s, 2H, −CH_2NMe$_3$), 3.01 (s, 9H, −N*Me*$_3$), 2.82 (br s, 2H, −CH_2CH$_2$NMe$_3$), 2.16 (s, 6H, ArCH_3), 2.11 (s, 6H, ArCH_3). ^{13}C NMR (DMSO-d_6, 100.61 MHz): δ 152.0, 130.7, 128.3, 127.4, 124.2, 122.3, 60.6, 53.9, 52.4, 44.7, 20.2, 16.3. HRMS: calcd. for $C_{23}H_{35}N_2O_2$ [M – Cl$^-$]$^+$ = 371.2699; found 371.2699.

Synthesis of 2−(bis(2−hydroxy−3,5−dimethylbenzyl)amino−*N*,*N*,*N*−trimethylethan-1-aminium nitrate (12). The desired product **12** (0.65 g, 75 %) as a beige powder was prepared by reacting compound **4** (0.99 g, 2.0 mmol) with silver nitrate (0.37 g, 2.2 mmol) in a manner analogous to the procedure for compound **10**; mp 155.3−157.6 °C; ^{1}H NMR (DMSO-d_6, 400.13 MHz): δ 8.96 (s, 2H, −O*H*), 6.84 (s, 2H, Ar−*H*), 6.80 (s, 2H, Ar−*H*), 3.68 (s, 4H, PhCH_2N−), 3.59 (m, 2H, −CH_2NMe$_3$), 2.98 (s, 9H, −N*Me*$_3$), 2.82 (t, 2H, J = 7.6 Hz, −CH_2CH$_2$NMe$_3$), 2.17 (s, 6H, ArCH_3), 2.12 (s, 6H, ArCH_3). ^{13}C NMR (DMSO-d_6, 100.61 MHz): δ 152.0, 130.7, 128.2, 127.4, 124.2, 122.3, 60.8, 53.9, 52.4, 44.9, 20.1, 16.2. HRMS: calcd. for $C_{23}H_{35}N_2O_2$ [M − NO$_3^-$]$^+$ = 371.2699; found 371.2693.

Synthesis of *N*−benzyl−2−(bis(2−hydroxy−3,5−dimethylbenzyl)amino)−*N*,*N*−dimethylethan−1−aminium bromide (13). The desired product **13** (1.5 g, 93 %) as a colorless solid was prepared by reacting compound **3** (1.1 g, 3.0 mmol) with benzyl bromide (1.0 g, 3.0 mmol) in a manner analogous to the procedure for **2**; mp 195.6−198.3 °C; ^{1}H NMR ($CDCl_3$, 500.13 MHz): δ 8.21 (s, 2H, −OH), 7.38 (m, 5H, −NMe$_2$CH$_2$*Ph*), 6.86 (s, 2H, Ar−*H*), 6.71 (s, 2H, Ar−*H*), 4.75 (s, 4H, −NMe$_2$CH_2Ph), 3.88 (t, 2H, J = 6.7 Hz, −CH_2NCH$_2$Ph), 3.77 (s, 4H, ArCH_2N−), 3.04 (s, 6H, −N*Me*$_2$CH$_2$Ph), 2.94 (t, 2H, J = 6.4 Hz, −NCH_2CH$_2$NCH$_2$Ph), 2.22 (s, 6H, ArCH_3), 2.18 (s, 6H, ArCH_3). ^{13}C NMR ($CDCl_3$, 125.76 MHz): δ 152.0, 133.1, 131.6, 130.8, 129.2, 128.9, 128.7, 126.7, 125.4, 121.4, 67.9, 61.6, 55.9, 49.7, 45.1, 20.4, 16.6. HRMS: calcd. for $C_{29}H_{39}N_2O_2$ [M – Br$^-$]$^+$ = 447.3006; found 447.3007.

Synthesis of *N*−benzyl−2−(bis(2−hydroxy−3,5−dimethylbenzyl)amino)−*N*,*N*−dimethylethan−1−aminium chloride (14). The desired product **14** (0.76 g, 79 %) as a colorless solid was prepared by reacting compound **3** (1.1 g, 3.0 mmol) with benzyl chloride (0.76 g, 6.0 mmol) in a manner analogous to the procedure for **2**; mp 180.4−183.7 °C; ^{1}H NMR ($CDCl_3$, 400.13 MHz): δ 8.76 (s, 2H, −OH), 7.34 (m, 5H, −NMe$_2$CH$_2$*Ph*), 6.85 (s, 2H, Ar−*H*), 6.69 (s, 2H, Ar−*H*), 4.71 (s, 2H, −NMe$_2$CH_2Ph), 3.89 (t, 2H, J = 6.5 Hz, −CH_2NCH$_2$Ph), 3.76 (s, 4H, ArCH_2N−), 3.05 (s, 6H, −N*Me*$_2$CH$_2$Ph), 2.93 (t, 2H, J = 6.7 Hz, −NCH_2CH$_2$NCH$_2$Ph), 2.22 (s, 6H, ArCH_3), 2.18 (s, 6H, ArCH_3). ^{13}C NMR ($CDCl_3$, 125.76 MHz): δ 152.1, 133.0, 131.5, 130.7, 129.2, 128.8, 128.7, 126.8, 125.8, 121.7, 67.9, 61.3, 55.8, 49.8, 45.1, 20.4, 16.6. HRMS: calcd. for $C_{29}H_{39}N_2O_2$ [M – Cl$^-$]$^+$ = 447.3006; found 447.3006.

Synthesis of 2−(bis(2−hydroxy−5−nitrobenzyl)amino)−*N*,*N*,*N*−trimethylethan−1−aminium iodide (15). The desired product **15** (1.2 g, 83 %) as a pale yellow solid was prepared by reacting 2,2'−(((2−(dimethylamino)ethyl)azanediyl)bis(methylene))bis(4−nitrophenol) (1.17 g, 3.0 mmol) with methyl iodide (1.7 g, 12 mmol) in a manner analogous to the procedure for **2**; mp 210.6−213.5 °C; ^{1}H NMR (DMSO-d_6, 400.13 MHz): δ 11.28 (br s, 2H, −OH), 8.20 (d, 2H, J = 2.9 Hz, Ar−*H*), 8.01 (dd, 2H, J_1 = 6.5 Hz, J_2 = 2.9 Hz, Ar−*H*), 6.96 (d, 2H, J = 9.0 Hz, Ar−*H*), 3.73 (s, 4H, ArCH_2N−), 3.60 (t, 2H, J = 6.9 Hz, −NCH$_2$CH_2NMe$_3$), 3.05 (s, 9H, −NMe_3), 2.96 (t, 2H, J = 6.7 Hz, −NCH_2CH$_2$NMe$_3$). ^{13}C NMR (DMSO-d_6, 100.61 MHz): δ 162.2, 139.4, 126.0, 125.3, 124.7, 115.3, 61.6, 52.6, 51.8, 47.2. HRMS: calcd. for $C_{19}H_{25}N_4O_6$ [M – I$^-$]$^+$ = 405.1769; found 405.1769.

Synthesis of 2−(bis(5−bromo−2−hydroxybenzyl)amino)−*N*,*N*,*N*−trimethylethan−1−aminium iodide (16). A solution of 4−bromophenol (8.7 g, 50 mmol), *N*,*N*−dimethylethylenediamine (2.2 g, 25 mmol), and 36% aqueous formaldehyde (4.1 g, 50 mmol) was stirred in refluxing methanol for 72 h. The mixture was cooled, and the product was filtered and washed with ice cold methanol. All volatiles were then removed *in vacuo* to give 2,2'−(((2−(dimethylamino)ethyl)azanediyl)bis(methylene))bis(4−bromophenol) (5.3 g, 46 %) as a colorless solid; mp 167.5−168.3 °C; ^{1}H NMR (CDCl$_3$, 400.13 MHz): δ 10.04 (br s, 2H, −OH), 7.24 (dd, 2H, J_1 = 2.0 Hz, J_2 = 2.4 Hz, Ar−*H*), 7.12 (d, 2H, J = 1.9 Hz, Ar−*H*), 6.73 (d, 2H, J = 8.6 Hz, Ar−*H*), 3.56 (s, 4H, ArCH_2N−), 2.60 (m, 4H, − CH_2CH_2NMe$_2$), 2.29 (s, 6H, −NMe_2). ^{13}C NMR (CDCl$_3$, 100.61 MHz): δ 156.1, 132.5, 132.3, 124.2, 118.8, 110.8, 55.9, 55.3, 49.1, 44.8. HRMS: calcd. for $C_{18}H_{23}Br_2N_2O_2$ [M + H] = 457.0126; found 457.0122. The desired product **16** (1.44 g, 80 %) as a pale yellow solid was prepared by reacting 2,2'−(((2−(dimethylamino)ethyl)azanediyl)bis(methylene))bis(4−bromophenol) (1.37 g, 3.0 mmol) with methyl iodide (1.7 g, 12 mmol) in a manner analogous to the procedure for **2**; mp 218.3−219.5 °C; ^{1}H NMR (CDCl$_3$, 400.13 MHz): δ 9.96 (br s, 2H, −OH), 7.41 (s, 2H, Ar−*H*), 7.26 (dd, 2H, J_1 = 6.15 Hz, J_2 = 2.4 Hz, Ar−*H*), 6.79 (d, 2H, J = 8.55 Hz, Ar−*H*), 3.62 (s, 4H, ArCH_2N−), 3.57 (t, 2H, J_1 = 6.15 Hz, −CH_2NMe$_2$), 3.01 (s, 9H, −NMe_2) , 2.83 (t, 2H, J_1 = 6.45 Hz, −CH_2CH$_2$NMe$_2$). ^{13}C NMR (DMSO-d_6, 100.61 MHz): δ 155.2, 132.5, 130.8, 126.3, 117.3, 110.0, 61.4, 52.5, 51.7, 46.1. HRMS: calcd. for $C_{19}H_{25}Br_2N_2O_2^+$ [M – I$^-$]$^+$ = 471.0277; found 471.0276.

Synthesis of 2−(bis(2−hydroxybenzyl)amino)−*N*,*N*,*N*−trimethylethan−1−aminium iodide (17). The desired product **17** (1.19 g, 90 %) as a pale yellow solid was prepared by reacting 2,2'−(((2−(dimethylamino)ethyl)azanediyl)bis(methylene))diphenol (0.9 g, 3.0 mmol) with methyl iodide (1.7 g, 12 mmol) in a manner analogous to the procedure for **2**; mp 81.8−84.9 °C; ^{1}H NMR (CD$_3$CN, 400.13 MHz): δ 8.60 (br s, 2H, −OH), 7.19 (m, 4H, Ar−*H*), 6.86 (m, 4H, Ar−*H*), 3.80 (s, 4H, ArCH_2N−), 3.46 (t, 2H, J = 7.75 Hz, −CH_2NMe$_3$), 2.94 (m, 11H, −NMe_3 and −NCH_2CH$_2$NMe$_3$). ^{13}C NMR (CD$_3$CN, 100.61 MHz): δ 157.6, 131.9, 130.4, 123.4, 120.8, 116.9, 63.5, 55.7, 54.4, 46.5. HRMS: calcd. for $C_{19}H_{27}N_2O_2^+$ [M – I$^-$]$^+$ = 315.2073; found 315.2067.

Synthesis of 2−(bis(5−(*tert*−butyl)−2−hydroxybenzyl)amino)−*N*,*N*,*N*−trimethylethan−1−aminium iodide (18). A solution of 4−*tert*−butylphenol (7.5 g, 50 mmol), *N*,*N*−dimethylethylenediamine (2.2 g, 25 mmol), and 36% aqueous formaldehyde (4.1 g, 50 mmol) was stirred in refluxing methanol for 24 h. The mixture was cooled, and the product was filtered and washed with ice cold methanol. All volatiles were then removed *in vacuo* to give 2,2'−(((2−(dimethylamino)ethyl)azanediyl)bis(methylene))bis(4−*tert*−butyl)phenol) (9.2 g, 89 %) as a colorless solid; mp 166.8−167.6 °C; ^{1}H NMR (CDCl$_3$, 400.13 MHz): δ 9.82 (s, 2H, −O*H*), 7.20 (dd, 2H, J_1 = 6.0 Hz, J_2 = 2.4 Hz, Ar−*H*), 7.04 (d, 2H, J = 2.4 Hz, Ar−*H*), 6.83 (d, 2H, J = 8.5 Hz, Ar−*H*), 3.65 (s, 4H, ArCH_2N−), 2.63 (m, 4H, −CH_2CH_2NMe$_2$), 2.33 (s, 6H, −NMe_2), 1.29 (s, 18H, ArC(CH_3)$_3$). ^{13}C NMR (CDCl$_3$, 100.61 MHz): δ 155.8, 137.1, 128.3, 126.4, 122.6, 118.0, 56.0,

55.7, 48.9, 44.7, 34.8, 29.4. HRMS: calcd. for $C_{26}H_{40}N_2O_2$ [M + H] = 413.3168; found 413.3167. The desired product **18** (1.5 g, 89 %) as a pale yellow solid was prepared by reacting 2,2'−(((2−(dimethylamino)ethyl)azanediyl)bis(methylene))bis(4−*tert*−butyl)phenol) (1.23 g, 3.0 mmol) with methyl iodide (1.7 g, 12 mmol) in a manner analogous to the procedure for **2**; mp 115.8−118.2 °C; ^{1}H NMR (DMSO-d_6, 400.13 MHz): δ 9.40 (s, 2H, −O*H*), 7.23 (s, 2H, Ar−*H*), 7.12 (d, 2H, J = 7.5 Hz, Ar−*H*), 6.76 (d, 2H, J = 8.3 Hz, Ar−*H*), 3.63 (s, 4H, ArCH_2−), 3.54 (br s, 2H, −CH_2NMe$_3$), 2.95 (s, 9H, −N*Me*$_3$), 2.79 (br s, 2H, −NCH_2CH$_2$NMe$_3$), 1.23 (s, 18H, ArC(CH_3)$_3$). ^{13}C NMR (DMSO-d_6, 100.61 MHz): δ 153.6, 141.0, 127.2, 124.9, 122.6, 114.8, 61.2, 52.4, 52.2, 45.9, 31.7, 31.4. HRMS: calcd. for $C_{27}H_{43}N_2O_2$ [M – I$^-$]$^+$ = 427.3319; found 427.3319.

Synthesis of 2−(bis(2−hydroxy−5−methoxybenzyl)amino)−*N*,*N*,*N*−trimethylethan−1−aminium iodide (19). The desired product **19** (1.41 g, 94 %) as a pale yellow solid was prepared by reacting 2,2'−(((2−(dimethylamino)ethyl)azanediyl)bis(methylene))bis(4−methoxyphenol) (1.08 g, 3.0 mmol) with methyl iodide (1.7 g, 12 mmol) in a manner analogous to the procedure for **2**; mp 113.8−116.3 °C; ^{1}H NMR (DMSO-d_6, 400.13 MHz): δ 9.19 (s, 2H, −O*H*), 6.85 (d, 2H, J = 7.9 Hz, Ar−*H*), 6.75 − 6.68 (m, 4H, Ar−*H*), 3.65 (s, 6H, ArOCH_3), 3.63 (s, 4H, ArCH_2N−), 3.57 (t, 2H, J = 6.5 Hz, −CH_2NMe$_3$), 3.00 (s, 9H, −N*Me*$_3$), 2.82 (t, 2H, J = 6.4 Hz,, −NCH_2CH$_2$NMe$_3$). ^{13}C NMR (DMSO-d_6, 100.61 MHz): δ 152.0, 149.7, 124.2, 115.8, 115.8, 113.5, 61.2, 55.4, 52.5 (2C), 45.9. HRMS: calcd. for $C_{21}H_{31}N_2O_4$ [M – I$^-$]$^+$ = 375.2278; found 375.2278.

Synthesis of 2−(bis(5−(dimethylamino)−2−hydroxybenzyl)amino)−*N*,*N*,*N*−trimethylethan−1−aminium iodide (20). A solution of 4−dimethylaminophenol (6.9 g, 50 mmol), *N*,*N*−dimethylethylenediamine (2.2 g, 25 mmol), and 36% aqueous formaldehyde (4.1 g, 50 mmol) was stirred in refluxing methanol for 24 h. The mixture was cooled, and the product was filtered and washed with ice cold methanol. All volatiles were then removed *in vacuo* to give 2,2'−(((2−(dimethylamino)ethyl)azanediyl)bis(methylene))bis(4−(dimethylamino)phenol) (9.2 g, 89 %) as a colorless solid; mp 188.4−190.3 °C; ^{1}H NMR ($CDCl_3$, 400.13 MHz): δ 9.27 (s, 2H, −O*H*), 6.78 (d, 2H, J = 8.8 Hz, Ar−*H*), 6.65 (m, 2H, Ar−*H*), 6.50 (d, 2H, J = 3 Hz, Ar−*H*), 3.59 (s, 4H, ArCH_2N−), 2.80 (s, 12H, Ar−N*Me*$_2$), 2.58 (m, 4H, −CH_2CH_2NMe$_2$), 2.26 (s, 6H, −N*Me*$_2$). ^{13}C NMR ($CDCl_3$, 100.61 MHz): δ 149.0, 144.5, 122.8, 117.2, 116.3, 115.3, 56.2, 56.1, 49.1, 44.8, 42.1. HRMS: calcd. for $C_{22}H_{35}N_4O_2$ [M + H] = 387.2760; found 387.2755.

2,2'−(((2−(dimethylamino)ethyl)azanediyl)bis(methylene))bis(4−(dimethylamino)phenol) (1.16 g, 3.0 mmol) was dissolved in dichloromethane (10 mL) and cooled to −78°C. stirring, methyl iodide in dichloromethane (0.43 g, 3 mmol in 5 mL) was added over 30 minutes with a dropping funnel. After stirring at −78°C for 1 h, the mixture was allowed to warm to room temperature over 2 hours. all volatiles were removed at reduced pressure. The obtained crude solids were washed with diethyl ether (3 × 40 mL). All volatiles were then removed *in vacuo* to give the desired product **20** (1.52 g, 96 %) as a colorless solid; mp 111.1−113.6 °C; ^{1}H NMR (DMSO-d_6, 400.13 MHz): δ 7.86 (d, 2H, J = 3.85 Hz, Ar−*H*), 7.69 (dd, 2H, J_1 = 5.8 Hz, J_2 = 3.32 Hz, Ar−*H*), 6.95 (d, 2H, J = 11.3 Hz, Ar−*H*), 3.75 (s, 4H, ArCH_2N−), 3.64 (t, 2H, J = 6.4 Hz, −CH_2NMe$_3$), 3.56 (s, 12H, Ar−N*Me*$_2$), 3.03 (s, 9H, −N*Me*$_3$) 2.87 (t, 2H, J = 6.4 Hz, −NCH_2CH$_2$NMe$_3$). ^{13}C NMR (DMSO-d_6, 100.61 MHz): δ 156.6, 138.6, 124.9, 122.4, 120.6, 115.6, 61.1, 56.7, 52.6, 52.4, 46.1. HRMS: calcd. for $C_{23}H_{37}N_4O_2$ [M – I$^-$]$^+$ = 401.2911; found 401.2911.

Computational Details. All calculations were performed based on density functional theory (DFT)[23] win the Jaguar 9.1 suite[37] at M06-D3[38,39] levels of theory. The optimization of every structures were carried out with the 6-31G** basis set, with the relativistic effective core potential containing Los Alamos LACVP basis set.[40–42] After the geometry optimization, the

energies of the optimized structures were recalculated with a high quality triple-ζ basis set cc-pVTZ(-f).[43] All atoms in the complexes were treated with LACV3P** basis set, which are one of the classes in LACVP basis functions where the exponents were decontracted to match with the triple-ζ functions of the main group elements. Vibrational frequencies for the optimized structures were calculated at the same level of theory as the geometry optimization. Calculated vibrational entropy correction along with the zero point vibrational energies were considered for proper thermodynamic approximations. At last, based on the optimized gas phase geometries, solvation correction energies were deduced. Self-consistent reaction field (SCRF)[44–46] approximations were considered to calculate the linearized Poisson-Boltzmann equations with the dielectric constant ε. The solvation energy used in the catalytic system was treated with propylene oxide (ε = 16.0).

ASSOCIATED CONTENT

Supporting Information

The Supporting Information is available free of charge on the ACS Publications website. Computational details and Cartesian coordinates of all computed structures and copies of the ^{1}H and ^{13}C NMR spectra and EIMS for all new products (PDF). Single-crystal X-ray data for compound **4** (cif).

AUTHOR INFORMATION

Corresponding Authors

*mbaik2805@kaist.ac.kr, *ykim@chungbuk.ac.kr

ORCID

Mu-Hyun Baik: 0000-0002-8832-8187

Youngjo Kim: 0000-0001-8571-0623

Author Contributions

#M.H. and Y.K. contributed equally to this work.

Notes

The authors declare no competing financial interests.

ACKNOWLEDGMENTS

Y.K gratefully acknowledge financial support from the National Research Foundation of Korea (NRF) grant funded by the Korea government (MSIT) (No. 2018R1A2B6004037). M.-H.B. acknowledges support from the Institute for Basic Science (IBS-R10-D1) in Korea.

REFERENCES

1 Leung, D. Y. C.; Caramanna, G.; Maroto-Valer, M. M. An overview of current status of carbon dioxide capture and storage technologies. *Renew. Sust. Energ. Rev.* **2014**, *39*, 426.

2 (a) Sakakura, T.; Choi, J.-C.; Yasuda, H. Transformation of carbon dioxide. *Chem. Rev.* **2007**, *107*, 2365. (b) Liu, Q.; Wu, L.; Jackstell, R.; Beller, M. Using carbon dioxide as a building block in organic synthesis. *Nat. Commun.* **2015**, *6*, 5933. (c) Yang, Z.-Z.; He, L.-N.; Gao, J.; Liu, A.-H.; Yu, B. Carbon dioxide utilization with C–N bond formation: carbon dioxide capture and subsequent conversion. *Energy Environ. Sci.* **2012**, *5*, 6602. (d) Tlili, A.; Blondiaux, E.; Frogneux, X.; Cantat, T. Reductive functionalization of CO_2 with amines: an entry to formamide, formamidine and methylamine derivatives. *Green Chem.* **2015**, *17*, 157.

3 (a) Omae, I. Recent developments in carbon dioxide utilization for the production of organic chemicals. *Coord. Chem. Rev.* **2012**, *256*, 1384. (b) Maeda, C.; Miyazaki, Y.; Ema, T. Recent progress in catalytic conversions of carbon dioxide. *Catal. Sci. Technol.* **2014**, *4*, 1482.

4 Roshan, S. N.; Zhang, Y. Recent developments in carbon dioxide utilization under mild conditions. *Dalton Trans.* **2010**, *39*, 3347.

5 Adhikari, D.; Miller, A. W.; Baik, M.-H.; Nguyen, S. T. Intramolecular ring-opening from a CO_2-derived nucleophile as the origin of selectivity for 5-substituted oxazolidinone from the (salen)Cr-catalyzed [aziridine + CO_2] coupling. *Chem. Sci.* **2015**, *6*, 1293.

6 North, M.; Pasquale, R.; Young, C. Synthesis of cyclic carbonates from epoxides and CO_2. *Green Chem.* **2010**, *12*, 1514.

7 Martín, C.; Fiorani, G.; Kleij, A. W. Recent advances in the catalytic preparation of cyclic organic carbonates. *ACS Catal.* **2015**, *5*, 1353.

8 (a) Comerford, J. W.; Ingram, I. D. V.; North, M.; Wu, X. Sustainable metal-based catalysts for the synthesis of cyclic carbonates containing five-membered rings. *Green Chem.* **2015**, *17*, 1966. (b) Narang, S.; Mehta, R.; Upadhyay, S. N. Copolymerization of propylene oxide and carbon dioxide. *Curr. Org. Chem.* **2015**, *19*, 2344.

9 (a) Castro–Osma, J. A.; North, M.; Wu, X. Synthesis of cyclic carbonates catalysed by chromium and aluminium salphen complexes. *Chem. Eur. J.* **2016**, *22*, 2100. (b) Maeda, C.; Shimonishi, J.; Miyazaki, R.; Hasegawa, J.; Ema, T. Highly active and robust metalloporphyrin catalysts for the synthesis of cyclic carbonates from a broad range of epoxides and carbon dioxide. *Chem. Eur. J.* **2016**, *22*, 6556. (c) Taherimehr, M.; Decortes, A.; Al-Amsyar, S. M.; Lu-eangchaichaweng, W.; Whiteoak, C. J.; Escudero–Adán, E. C.; Kleij, A. W.; Pescarmona, P. P. A highly active Zn(salphen) catalyst for production of organic carbonates in a green CO_2 medium. *Catal. Sci. Technol.* **2012**, *2*, 2231. (d) Castro–Osma, J. A.; Alonso-Moreno, C.; Lara–Sánchez, A.; Martinez, J.; North, M.; Otero, A. Synthesis of cyclic carbonates catalysed by aluminium heteroscorpionate complexes. *Catal. Sci. Technol.* **2014**, *4*, 1674.

10 (a) Cokoja, M.; Wilhelm, M. E.; Anthofer, M. H.; Herrmann, W. A.; Kühn, F. E. Synthesis of cyclic carbonates from epoxides and carbon dioxide by using organocatalysts. *ChemSusChem* **2015**, *8*, 2436. (b) Fiorani, G.; Guo, W.; Kleij, A. W. Sustainable conversion of carbon dioxide: the advent of organocatalysis. *Green Chem.* **2015**, *17*, 1375.

11 Sopeña, S.; Fiorani, G.; Martín, C.; Kleij, A. W. Highly efficient organocatalyzed conversion of oxiranes and CO_2 into organic carbonates. *ChemSusChem* **2015**, *8*, 3248.

12 (a) Martínez-Rodríguez, L.; Garmilla, J. O.; Kleij, A. W. Cavitand-based polyphenols as highly reactive organocatalysts for the coupling of carbon dioxide and Oxiranes. *ChemSusChem* **2016**, *9*, 749. (b) Wang, J.-Q.; Sun,

J.; Cheng, W.-G.; Dong, K.; Zhang, X.-P.; Zhang, S.-J. Experimental and theoretical studies on hydrogen bond-promoted fixation of carbon dioxide and epoxides in cyclic carbonates. *Phys. Chem. Chem. Phys.* **2012**, *14*, 11021.

13 (a) Whiteoak, C. J.; Henseler, A. H.; Ayats, C.; Kleij, A. W.; Pericàs, M. A. Conversion of oxiranes and CO_2 to organic cyclic carbonates using a recyclable, bifunctional polystyrene-supported organocatalyst. *Green Chem.* **2014**, *16*, 1552. (b) Jose, T.; Cañellas, S.; Pericàs, M. A.; Kleij, A. W. Polystyrene-supported bifunctional resorcinarenes as cheap, metal-free and recyclable catalysts for epoxide/CO_2 coupling reactions. *Green Chem.* **2017**, *19*, 5488. (c) Büttner, H.; Lau, K.; Spannenberg, A.; Werner, T. Bifunctional one-component catalysts for the addition of carbon dioxide to epoxides. *ChemCatChem* **2015**, *7*, 459.

14 Büttner, H.; Steinbauer, J.; Werner, T. Synthesis of cyclic carbonates from epoxides and carbon dioxide by using bifunctional one-component phosphorus-based organocatalysts. *ChemSusChem* **2015**, *8*, 2655.

15 Werner, T.; Büttner, H. Phosphorus-based bifunctional organocatalysts for the addition of carbon dioxide and epoxides. *ChemSusChem* **2014**, *7*, 3268.

16 Liu, S.; Suematsu, N.; Shirakawa, S. Design of bifunctional quaternary phosphonium salt catalysts for CO_2 fixation reaction with epoxides under mild conditions. *Green Chem.* **2016**, *18*, 4611.

17 Büttner, H.; Steinbauer, J.; Wulf, C.; Dindaroglu, M.; Schmalz, H.; Werner, T. Organocatalyzed synthesis of oleochemical carbonates from CO_2 and renewables. *ChemSusChem* **2017**, *10*, 1076.

18 Whiteoak, C. J.; Nova, A.; Maseras, F.; Kleij, A. W. Merging sustainability with organocatalysis in the formation of organic carbonates by using CO_2 as a feedstock. *ChemSusChem* **2012**, *5*, 2032.

19 Hardman-Baldwin, A. M.; Mattson, A. E. Silanediol-catalyzed carbon dioxide fixation. *ChemSusChem* **2014**, *7*, 3275.

20 Zhou, H.; Wang, G.-X.; Zhang, W.-Z.; Lu, X.-B. CO_2 Adducts of phosphorus ylides: highly active organocatalysts for carbon dioxide transformation. *ACS Catal.* **2015**, *5*, 6773.

21 Wang, L.; Zhang, G.; Kodama, K.; Hirose, T. An efficient metal- and solvent-free organocatalytic system for chemical fixation of CO2 into cyclic carbonates under mild conditions. *Green Chem.* **2016**, *18*, 1229.

22 (a) Kim, S. H.; Ahn, D.; Kang, Y. Y.; Kim, M.; Lee, K.-S.; Lee, J.; Park, M. H.; Kim, Y. Zirconocene complexes as catalysts for the cycloaddition of CO_2 to propylene oxide. *Eur. J. Inorg. Chem.* **2014**, *30*, 5107. (b) Melendez, J.; North, M.; Pasquale, R. Synthesis of cyclic carbonates from atmospheric pressure carbon dioxide using exceptionally active aluminium(salen) complexes as catalysts. *Eur. J. Inorg. Chem.* **2007**, *21*, 3323. (c) Paddock, R. L.; Nguyen, S. T. Chemical CO_2 Fixation: Cr(III) salen complexes as highly efficient catalysts for the coupling of CO_2 and epoxides. *J. Am. Chem. Soc.* **2001**, *123*, 11498. (d) Castro-Osma, J. A.; Lamb, K. J.; North, M. Cr(salophen) Complex catalyzed cyclic carbonate synthesis at ambient temperature and pressure. *ACS Catal.* **2016**, *6*, 5012. (e) Ohkawara, T.; Suzuki, K.; Nakano, K.; Mori, S.; Nozaki, K. Facile estimation of catalytic activity and selectivities in copolymerization of propylene oxide with carbon dioxide mediated by metal complexes with planar tetradentate ligand. *J. Am. Chem. Soc.* **2014**, *136*, 10728. (f) Nakano, K.; Kamada, T.; Nozaki, K. Selective formation of polycarbonate over cyclic carbonate: Copolymerization of epoxides with carbon dioxide catalyzed by a cobalt(III) complex with a piperidinium end-capping arm. *Angew. Chem., Int. Ed.* **2006**, *45*, 7274.

23 Parr, R. G.; Yang, W. Density functional theory of atoms and molecules; Oxford University Press: New York, 1989.

24 (a) Wang, J.; Zhang, Y. Boronic acids as hydrogen bond donor catalysts for efficient conversion of CO_2 into organic carbonate in water. *ACS Catal.* **2016**, *6*, 4871. (b) Taheri, M.; Ghiaci, M.; Shchukarev, A. Cross-linked chitosan with a dicationic ionic liquid as a recyclable biopolymer-supported catalyst for cycloaddition of carbon dioxide with epoxides into cyclic carbonates. *New J. Chem.* **2018**, *42*, 587. (c) Arayachukiat, S.; Kongtes, C.; Barthel, A.; Vummaleti, S. V. C.; Poater, A.; Wannakao, S.; Cavallo, L.; D'Elia, V. Ascorbic acid as a bifunctional hydrogen bond donor for the synthesis of cyclic carbonates from CO_2 under ambient conditions. *ACS Sustainable Chem. Eng.* **2017**, *5*, 6392. (d) Duval, A.; Averous, L. Cyclic carbonates as safe and versatile etherifying reagents for the functionalization of lignins and tannins. *ACS Sustainable Chem. Eng.* **2017**, *5*, 7334.

25 Kim, S. H.; Ahn, D.; Go, M. J.; Park, M. H.; Kim, M.; Lee, J.; Kim, Y. Dinuclear aluminum complexes as catalysts for cycloaddition of CO_2 to epoxides. *Organometallics* **2014**, *33*, 2770.

26 Tshuva, E. Y.; Goldberg, I.; Kol, M.; Goldschmidt, Z. Zirconium complexes of amine−bis(phenolate) ligands as catalysts for 1-hexene polymerization: Peripheral structural parameters strongly affect reactivity. *Organometallics* **2001**, *20*, 3017.

27 Hansch, C.; Leo, A.; Taft, R. W. A survey of Hammett substituent constants and resonance and field parameters. *Chem. Rev.* **1991**, *91*, 165.

28 Shriver, D. F.; Drezdzon, M. A. *The Manipulation of Air-Sensitive Compounds*, 2nd ed., Wiley, New York, 1986.

29 Girolami, G. S.; Rauchfuss, T. B.; Angelici, R. J. *Synthesis and Technique in Inorganic Chemistry*, 3rd ed., University Science Books, Sausalito, CA, 1999.

30 Armarego, W. L. F.; Chai, C. L. L. *Purification of Laboratory Chemicals*, 6th ed., Elsevier, New York, 2009.

31 Judmaier, M. E.; Holzer, C.; Volpe, M.; Mösch−Zanetti, N. C. Molybdenum(VI) dioxo complexes employing Schiff base ligands with an intramolecular donor for highly selective olefin epoxidation. *Inorg. Chem.* **2012**, *51*, 9956.

32 Lee, J.; Do, Y.; Kim, Y.; Park, D.Y.; Jeong, Y.i; Lee, M. Multinuclear half metallocene catalyst and method for preparing syndiotactic polystyrene using the same. Eur. Pat. Appl. (2007), EP 1777230 A1 20070425; *Chem. Abstr.* **2007**, *146*, 442290.

33 Velusamy, M.; Palaniandavar, M.; Gopalan, R. S.; Kulkarni. G. U. Novel iron(III) complexes of tripodal and linear tetradentate bis(phenolate) ligands: Close relevance to intradiol-cleaving catechol dioxygenases. *Inorg. Chem.* **2003**, *42*, 8283.

34 Hinshaw, C. J.; Peng, G.; Singh, R.; Spence, J. T.; Enemark, J. H.; Bruck, M.; Kristofiski, J.; Merbs, S. L.; Ortega, R. B.; Wexler, P. A. Molybdenum(VI)-dioxo complexes with linear and tripodal tetradentate ligands: models for the molybdenum(VI/V) centers of the molybdenum hydroxylases and related enzymes. 1. Syntheses and structures *Inorg. Chem.* **1989**, *28*, 4483.

35 Hirotsu, M.; Kojima, M.; Yoshikawa, Y. Mononuclear and mixed-valence trinuclear manganese complexes containing tripodal tetradentate ligands. Phenolato, carboxylato, and alkoxo bridges *Bull. Chem. Soc. Jpn.* **1997**, *70,* 649.

36 Bochevarov, A. D.; Harder, E.; Hughes, T. F.; Greenwood, J. R.; Braden, D. A.; Philipp, D. M.; Rinaldo, D.; Halls, M. D.; Zhang, J.; Friesner, R. A. Jaguar: A high-performance quantum chemistry software program with strengths in life and materials sciences. *Int. J. Quantum Chem.* **2013**, *113*, 2110.

37 Zhao, Y.; Truhlar, D. G. The M06 suite of density functionals for main group thermochemistry, thermochemical kinetics, noncovalent interactions, excited states, and transition elements: two new functionals and systematic testing of four M06-class functionals and 12 other functionals. *Theor. Chem. Acc.* **2008**, *120*, 215.

38 Grimme, S.; Antony, J.; Ehrlich, S.; Krieg, S. A consistent and accurate ab initio parametrization of density functional dispersion correction (DFT-D) for the 94 elements H-Pu. *J. Chem. Phys.* **2010**, *132*, 154104.

39 Hay, P. J.; Wadt, W. R. Ab initio effective core potentials for molecular calculations. Potentials for the transition metal atoms Sc to Hg. *J. Chem. Phys.* **1985**, *82*, 270.

40 Wadt, W. R.; Hay, P. J. Ab initio effective core potentials for molecular calculations. Potentials for main group elements Na to Bi. *J. Chem. Phys.* **1985**, *82*, 284.

41 Hay, P. J.; Wadt, W. R. Ab initio effective core potentials for molecular calculations. Potentials for K to Au including the outermost core orbitals. *J. Chem. Phys.* **1985**, *82*, 299.

42 Dunning, T. H., Jr. Gaussian basis sets for use in correlated molecular calculations. I. The atoms boron through neon and hydrogen. *J. Chem. Phys.* **1989**, *90*, 1007.

43 Marten, B.; Kim, K.; Cortis, C.; Friesner, R. A.; Murphy, R. B.; Ringnalda, M. N.; Sitkoff, D.; Honig, B. New model for calculation of solvation free energies: correction of self-consistent reaction field continuum dielectric theory for short-range hydrogen-bonding effects. *J. Phys. Chem.* **1996**, *100*, 11775.

44 Edinger, S. R.; Cortis, C.; Shenkin, P. S.; Friesner, R. A. Solvation Free Energies of Peptides: Comparison of approximate continuum solvation models with accurate solution of the Poisson−Boltzmann equation. *J. Phys. Chem. B* **1997**, *101*, 1190.

45 Friedrichs, M.; Zhou, R.; Edinger, S. R.; Friesner, R. A. Poisson−Boltzmann analytical gradients for molecular modeling calculations. *J. Phys. Chem. B* **1999**, *103*, 3057.

Table of Contents (TOC)

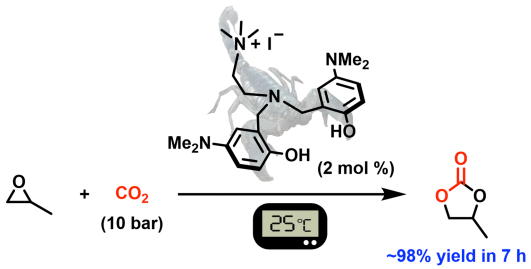

Highly Active, Versatile, Recyclable and Stable Scorpionate Organocatalyst